Energy & Buildings 346 (2025) 116189

Contents lists available at ScienceDirect

Energy & Buildings

journal homepage: www.elsevier.com/locate/enb

Climate change resilience of energy retrofit interventions in historic urban areas☆

Luigi Schibuola, Mauro De Paris, Paolo Di Micco, Davide Roncarati, Chiara Tambani *

University IUAV of Venice, Dorsoduro 2206, 30123 Venice, Italy

ARTICLE INFO

Keywords:
Historic urban center
Retrofit strategies
Renewable energy
Heat pump
PV system
SSP5-8.5
Climate change resilience

ABSTRACT

Decarbonizing the built environment has become a critical priority in addressing the impacts of climate change, necessitating comprehensive and effective energy retrofitting of existing buildings. Many historically significant cities feature urban centers rich in cultural and artistic heritage. Authorities impose restrictions on buildings under preservation order but must also assess retrofitting interventions on nearby non-protected structures to preserve the area's cultural integrity. In Padua, a historic area spanning 126,000 m2 was analyzed to identify the most effective energy retrofitting strategies, aiming to provide clear operational guidelines. A modeling approach based on building-plant system dynamic simulation of archetypes shows that interventions on building systems outperform those focused on building envelope insulation. Solar shading systems were incorporated in all retrofit scenarios, whereas other passive strategies were excluded due to their limited applicability in densely built and protected historical areas. Notably, the results highlight the highest energy savings achieved with heat pumps combined with photovoltaic systems, which are also less architecturally invasive, particularly when building-integrated photovoltaic systems and geothermal heat pumps are employed. Ultimately, the combined implementation of energy system measures and building envelope improvements resulted in energy savings of up to 83.9 % of the total energy consumption in the analyzed buildings. Thus, even buildings in historic areas can contribute significantly to achieving the energy transition goals set for 2050. A key factor in reaching this conclusion was the projection of the study into the SSP5-8.5 climate scenario for 2050, the most extreme pathway developed by the IPCC. Despite substantial differences in climate and in the energy behavior of buildings by 2050, new evaluations under this scenario confirmed the results obtained under current climate conditions. Consequently, the proposed intervention strategies remain effective through 2050, even under the most radical climate change projections.

1. Introduction

1.1. Overall overview

In the current context, buildings account for a significant share of energy consumption. According to data from the European Commission, 85 % of buildings in the European Union (EU) were constructed before 2000, and among these, 75 % exhibit poor energy performance [1,2]. The EU building stock is therefore responsible for 40 % of energy consumption and 36 % of greenhouse gas emissions [3,4]. Additionally, approximately 80 % of the energy used in EU buildings is allocated to heating, cooling, and domestic hot water production [5]. Addressing the energy efficiency of buildings is thus crucial to reducing energy consumption and lowering CO_2 emissions, which are the primary contributors to the greenhouse effect and climate change, exacerbating the planet's condition. The intensive use of fossil fuels undeniably contributes to the increasing concentration of greenhouse gases in the atmosphere. Buildings are particularly vulnerable to the effects of these changes.

The European Union is continuously seeking solutions to address the consequences of climate change [6,7]. With the introduction of the European Green Deal in 2019 [8–10], overarching goals were established to make the EU climate-neutral by 2050. These objectives entail the decarbonization of all economic sectors, including the building sector, and aim to foster an energy transition by redirecting the energy system toward renewable energy sources (RES).

Fit for 55 % [11–13]is a legislative package introduced by the

☆ This article is part of a special issue entitled: 'Decarbonising Built Env' published in Energy & Buildings.

* Corresponding author.
E-mail address: chiara.tambani@iuav.it (C. Tambani).

https://doi.org/10.1016/j.enbuild.2025.116189
Received 13 January 2025; Received in revised form 23 May 2025; Accepted 23 July 2025
Available online 28 July 2025

Nomenclature

Category symbols:

CR_A1950	Commercial-Residential buildings constructed before (Ante) 1950
CR_1950-75	Commercial-Residential buildings constructed between 1950 and 1975
CO_A1950	Commercial-Office buildings constructed before (Ante) 1950
CO_1950-75	Commercial-Office buildings constructed between 1950 and 1975
R_A1950	Residential buildings constructed before (Ante) 1950
R_1950-75	Residential buildings constructed between 1950 and 1975

Abbreviations:

ASHP	air source heat pump
BAPV	building-applied photovoltaics
BIPV	building-integrated photovoltaics
COP	coefficient of performance
DHW	domestic hot water
EER	energy efficiency ratio
EPBD	Energy Performance of Buildings Directive
EPW	energy plus weather
EU	European Union
EPS	expanded polyurethane
GHG	greenhouse gas
GWHP	ground water heat pump
HP	heat pump
HVAC	heating, ventilation and air conditioning
HDD	heating degree day
IPCC	Intergoverment Panel on Climate Change
PV	photovoltaic
RES	renewable energy source
SHC	solar heat gain coefficient
SSP	Shared Socioeconomic Pathway.

European Commission that sets binding targets to reduce greenhouse gas (GHG) emissions by 55 % by 2030 compared to 1990 levels, aligning with the Green Deal. The package includes a series of new or revised laws and regulations detailing how these targets will be achieved. These legislative tools translate the vision of the Green Deal into concrete measures [14,15].

The recast of the Energy Performance of Buildings Directive (EPBD) in May 2024 places significant emphasis on improving the energy performance of buildings and promoting low-GHG-emission buildings [16]. The 2024 EPBD sets clear energy-saving targets for residential buildings within the European Union. By 2030, member states must reduce energy consumption in residential buildings by 16 %, increasing to 20–22 % by 2035. To achieve the 16 % target by 2030, 55 % of this reduction must come from upgrading 43 % of the buildings currently performing at the lowest energy levels. This requires targeted interventions to improve the energy efficiency of the most energy-intensive buildings [17].

However, this directive does not apply to historic buildings under monument protection. Member states may choose to exclude buildings of significant architectural or historical value, temporary structures, churches, and places of worship, categories that require special consideration when addressing energy retrofitting or rehabilitation.

Energy efficiency in historic buildings has become a priority in urban sustainability policies, particularly in contexts characterized by high energy consumption and architectural conservation constraints [18,19]. For non-protected buildings in these areas, it remains essential to develop guidelines for potential energy retrofit interventions that consider the surrounding context [20]. The planning of energy retrofit strategies, however, requires an awareness of the actual benefits achievable through their implementation across various building typologies [21–23].

1.2. Foreseen scenarios: the shared socioeconomic pathways

In this context, the Shared Socioeconomic Pathways (SSPs) represent a valuable tool for investigating potential climate evolutions and their future implications. The SSPs are climate change scenarios projecting global socioeconomic changes up to 2100, as defined in the IPCC Sixth Assessment Report on climate change in 2021 [24,25]. They are employed to derive GHG emission scenarios under varying climate policies [26,27]. The SSPs provide narratives describing alternative socioeconomic developments.

The IPCC, the Intergovernmental Panel on Climate Change, has developed five SSPs ranging from the best-case scenario, with very low emissions, to the worst-case scenario, characterized by high levels of GHG emissions:

- SSP1-1.9: Global CO_2 emissions are low, reaching net zero around 2050, and global temperatures stabilize with an average increase of approximately +1.5 °C by 2100.
- SSP1-2.6: Global CO_2 emissions are significantly reduced, reaching net zero after 2050, and temperatures stabilize with an average increase of about +1.8 °C by the end of the century.
- SSP2-4.5: Emissions do not reach net zero by 2100, resulting in a temperature increase of approximately +2.7 °C.
- SSP3-7.0: Emissions double relative to current levels by 2100, leading to an average temperature increase of around +3.7 °C.
- SSP5-8.5: The worst-case scenario, where emissions double as early as 2050, causing an average temperature rise of about +4.4 °C by the end of the century.

These scenarios provide an analytical foundation for examining various growth and mitigation pathways, enabling insights into how ecological transition policies, including targeted interventions in the building sector, can help address global climate challenges [28]. Moreover, such analyses assist in evaluating the long-term effectiveness of interventions, even in a context of severe climatic deterioration [29,30].

1.3. Strategies towards building energy transition

To achieve the established objectives, it is essential to reduce building energy demand by improving the thermal insulation of the building envelope to minimize heat losses. This includes the addition of new and more efficient thermal insulation layers for opaque surfaces and enhancing the performance of windows and doors. These measures are complemented by the installation of high-efficiency heating, ventilation, and air conditioning (HVAC) systems [31,32]. A critical component is the thermal energy generation required for space heating, domestic hot water (DHW) production, and cooling for summer air conditioning. The use of heat pumps (HPs) powered by electricity allows for the provision of heating and cooling energy while eliminating the local emissions of GHGs typically associated with traditional boilers fueled by fossil fuels. Proper use of heat pumps can achieve energy savings compared to boilers, even with the widely used air source heat pumps (ASHPs) [33–36]. These energy advantages are further enhanced when alternative, more favorable thermal sources are utilized, such as surface water

[37–39], groundwater [40,41], or the ground itself through geothermal exchangers [42,43]. For this reason, as an alternative to ASHPs, this study considers the use of groundwater source heat pumps (GWHPs), which offer superior operating conditions due to the considerable thermal stability of groundwater throughout the year. This solution is viable in the analyzed study area, which is rich in both surface and groundwater resources.

The gradual increase in the use of renewable energy to meet building energy demands is a key requirement in current directives. In buildings, photovoltaic (PV) systems are currently the most widespread renewable energy technology, especially when paired with electric HPs, as the self-generated electricity can partially cover their consumption [44–47]. PV systems are typically installed on rooftops [32,48,49] and are often combined with electrical storage batteries to maximize the local use of produced electricity, extending it to periods of reduced or no photovoltaic generation.

This study considers two types of photovoltaic panels representative of Building-Applied Photovoltaics (BAPV) and Building-Integrated Photovoltaics (BIPV) [50,51].

- BAPV: These systems consist of PV modules installed on existing surfaces without altering the underlying building element. While effective in energy production, BAPV systems may pose aesthetic challenges, particularly for historic buildings, as the overlay of conventional modules on roof surfaces can compromise the visual and stylistic integrity [52].
- BIPV: This technology provides a more advanced and discreet solution, as PV systems are integrated directly into building elements, such as tiles, glass, or façades [53,54]. This approach significantly reduces visual impact and is, therefore, often more acceptable in historic contexts. BIPV modules can be designed to resemble traditional materials, such as tiles or stones, enabling better aesthetic integration with the building.

1.4. The aim of this study

This study evaluates the energy savings achievable through various retrofit technologies for the renovation of buildings not subject to protection but located in an urban area of high historical and monumental value. The selected area is in the city of Padua. A modeling approach based on archetypes was employed to assess the energy demand of the entire investigated area. The methodology involves categorizing the building stock and identifying representative building typologies based on characteristics influencing energy demand [55,56].

This approach enables the comparison of different retrofit strategies. The objective is to provide authorities responsible for developing intervention strategies with a classification of the effectiveness of various potential solutions, which can be implemented individually or in combination. This classification can guide the formulation of construction regulations to promote the most efficient interventions. To evaluate the energy performance of retrofitted buildings, dynamic simulation of the building-plant system was conducted using models developed with the DesignBuilder software [57], which employs EnergyPlus code as its calculation engine [58]. It is important to underline that the objective of this study is not to predict absolute energy consumption values but rather to provide a comparative evaluation of different retrofit strategies under standardized conditions. The use of carefully selected input data, based on national regulations and technical literature, along with a robust simulation methodology, ensures consistency and reliability in the comparative assessment of interventions.

A critical aspect of the analysis was the evaluation of how climate change affects the effectiveness of the examined retrofit solutions [59]. To address this, the study assesses the resilience of energy retrofit strategies, investigating their capacity to maintain high energy performance over time despite future climatic variations. By incorporating climate projections, this research establishes a structured framework for selecting interventions that ensure both long-term efficiency and the sustainability of historic urban areas. For this purpose, potential energy savings were assessed under different climatic conditions by comparing the current climate (2024) with the projected climate of 2050 under the worst-case scenario SSP5-8.5 [60]. Naturally, it is hoped that future decarbonization measures adopted by nations will mitigate the effects of the climate emergency. Likewise, the implementation of additional passive strategies will contribute to limiting the increase in cooling loads in buildings. The adoption of novel passive technologies must take into account the architectural constraints of existing structures within historic urban areas. To comprehensively assess the resilience of the proposed interventions, this study considers the worst case for these buildings in 2050. Unlike studies that focus on individual buildings or small-scale interventions, this research evaluates retrofit strategies across an extensive historic urban area, providing a broader and more applicable understanding of energy efficiency interventions at scale. The archetype-based approach enables the analysis of 42 different retrofit actions, both individually and in combination, offering a structured framework to assess their impact under both current and future climatic conditions. This study also contributes to urban energy planning by providing insights into the effectiveness of different strategies, helping decision-makers balance energy efficiency with heritage preservation.

The ultimate goal remains achieving climate neutrality by 2050, which entails eliminating all emissions caused by the use of fossil fuels for energy production. The challenge, therefore, lies in increasing the use of renewable energy sources to replace non-renewable ones. In this context, the focus on energy savings is not merely directed toward a general reduction in energy consumption but more specifically toward limiting the use of non-renewable energy, which must ultimately be reduced to zero [61]. This study thus aims to highlight not only the achievable energy savings but also the benefits in terms of reducing the demand for non-renewable energy sources.

2. Method

2.1. Area analysis and identification of archetype buildings

The studied area is shown in Fig. 1a. It is a densely built area located in the historical center of Padua. Initially, it was investigated based on the assessment already conducted by the Monumental Heritage Superintendence, which identified and excluded from the retrofit (and therefore from this study) all buildings subject to monumental protection. All remaining buildings were studied using GIS and the available cartography, which allowed for the creation of a detailed mapping of the area. For each of these buildings, the GIS provided essential dimensions, including height, number of floors, and plan layout. Consequently, the volumes were derived. On-site surveys, as well as the use of Google Maps, helped to determine the building usage types. The availability of historical maps allowed for the dating of the blocks. Based on the usage type, number of floors, and construction date, the buildings were classified into different categories. Starting from the usage type, eight categories were initially identified: Church (CH), Commercial (C), Commercial-Residential (CR), Commercial-Offices (CO), Warehouses (W), Residential (R), Public Services (PS), Commercial-Residential-Offices (CRO). Some categories were not analyzed because they consist of buildings subject to monumental protection. Ultimately, only three categories remained: R, CR, and CO. Regarding dating, reference was made to the periods indicated in the UNI TR 11552 standard [62] to identify the construction packages subsequently used for dynamic simulation. In our case, the periods to be used for the buildings in the area are limited to two: buildings constructed before (Ante) 1950 (A1950) and buildings constructed between 1950 and 1975 (1950–1975). Therefore, the categories actually analyzed are six.

In Fig. 1b, these six categories are highlighted, along with the buildings subject to monumental protection, which are not studied and are grouped under the category labeled MP. Subsequently, within each

a) b)

Fig. 1. Location of the investigated area within the urban fabric (a). In (b), a detailed view of the area with different building categories marked by colors.

category, the buildings were further divided into sub-categories based on the number of floors. This resulted in sub-categories that were named according to their three characteristics. For example, R_A1950_3P refers to a residential building, built before 1959, with 3 floors. For each sub-category, the volume share relative to the total volume of buildings in the respective category was also evaluated. The sub-category with the highest number of buildings was chosen as representative of the category, as highlighted in Fig. 2a with marking.

It was found that this sub-category also has the largest volumetric share among the buildings in a category, as shown in Fig. 2b, where this larger volumetric share is emphasized with larger font.

After identifying a representative sub-category for each category, the archetype buildings were determined by calculating the average volume. This was done by dividing the total volume of buildings in each selected sub-category by the number of buildings within that sub-category. The building chosen as the archetype is the one whose volume most closely approximates this average value. In Fig. 3, the volumes of the buildings belonging to each sub-category are shown, with the archetype building highlighted. For each sub-category, the volumetric average is also indicated by a bold horizontal line. At this point, the archetype is considered representative of the category. Thus, there are six archetype buildings corresponding to six categories, which allow for the study of the entire area.

2.2. Simulation model

For each archetype building, a simulation model was developed using the DesignBuilder software to evaluate the energy demand of the building in terms of hourly profiles for heating, cooling, and DHW demand, with the latter restricted to residential usage. Additionally, the model includes the energy demand for plug-in appliances and lighting. The six archetype buildings selected through the aforementioned procedure for simulation are highlighted in Fig. 4. The fundamental geometric characteristics of the six archetypes are reported in Table 1, while additional geometric details are provided in the Supplementary Material.

The modeling process required identifying the thermophysical characteristics of the building structures. For each category, typical structures from two historical periods represented in the studied area were considered: pre-1950 (A1950) and the period between 1950 and 1975 (1950–1975). The selection of construction packages was based on the Italian standard UNI TR 11552 [62], which specifies these construction characteristics according to the building age.

Table 2 presents the construction packages that will later undergo energy retrofitting, potentially distinguished by their historical period. It also includes the key general data necessary for the dynamic simulation of the buildings.

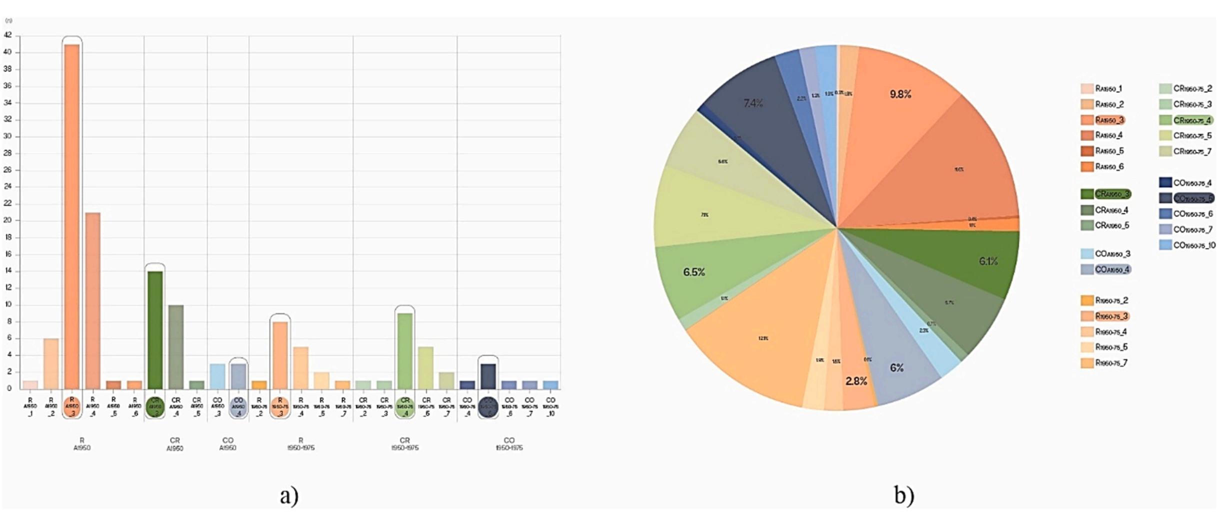

Fig. 2. Selection of the numerically most representative sub-categories (a), percentage volumetric incidence of each sub-category relative to the total building volume in the area (b).

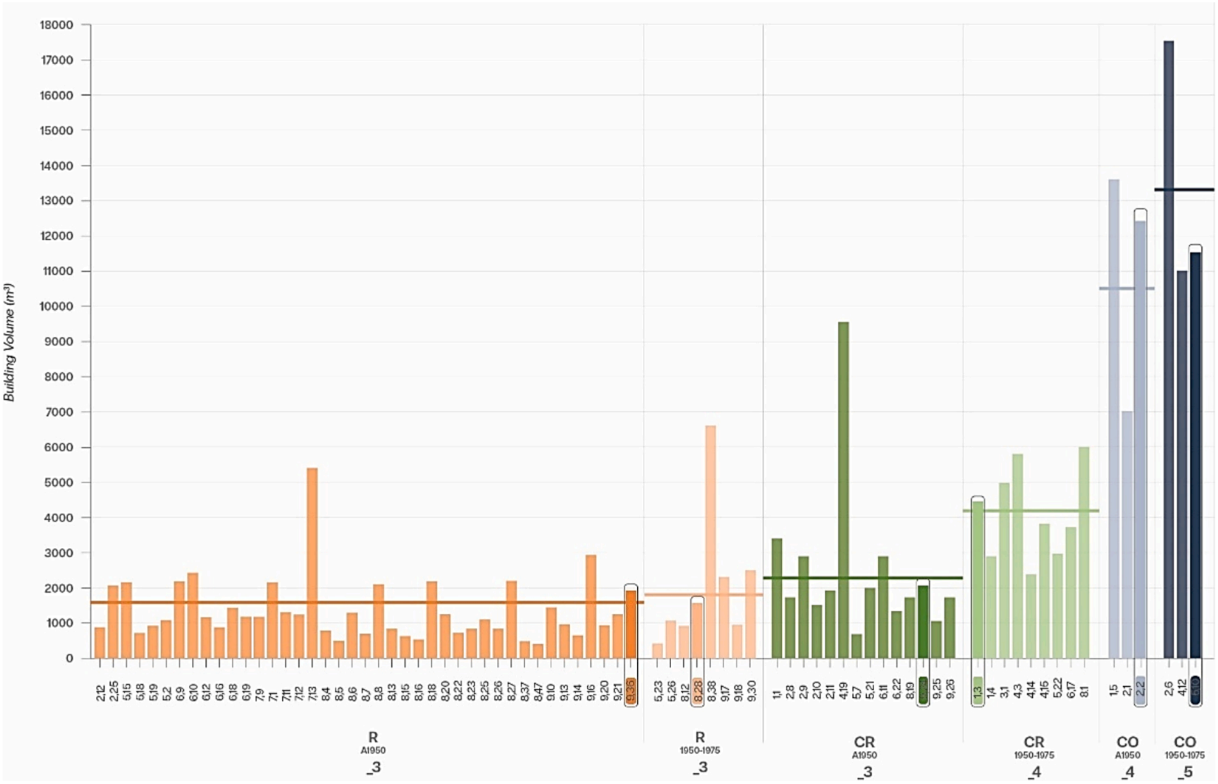

Fig. 3. Identification of the archetype building for each selected sub-category.

Fig. 4. The six archetypes identified for the study area.

Regarding the building systems analyzed in their existing state, the presence of outdated technologies was observed. Specifically, centralized heating systems with traditional boilers supplying a radiator-based heating network were identified. During the summer period, cooling is provided by air-cooled split systems.

Table 1
Geometric properties of the analyzed archetypes.

Archetype	Ground floor area (m^2)	Upper floors total area (m^2)	Total roof area (m^2)	Building height (m)	Window-to-floor ratio (%)	Total conditioned volume (m^3)
R_A1950_3	340.2	650.3	336.6	10.1	10.0	3339.7
R_1950-75_3	94.8	190.5	88.3	10.7	6.2	1017.3
CR_A1950_3	82.7	165.5	75.5	9.4	8.9	777.4
CR_1950-75_4	302.4	907,2	290.4	15.4	14.0	4656.9
CO_A1950_4	643.4	1751.6	580.2	19.1	5.8	11913.2
CO_1950-75_5	590.2	2050.7	581.3	16.9	18.1	8115.7

Table 2
Characteristics and simulation parameters of the archetypes.

Heating set point. (°C)	20
Cooling set point (°C)	26
Heating schedule (h)	7am-9pm[a] or 7am-7pm[b,c]
Cooling schedule (h)	11am-7am[a] or 9am-7pm[b,c]
DHW need (l/m^2day)	1.43[a]
DHW schedule	0 % (12am-6am), 30 % (6am-9am), 10 % (9am-12 pm), 15 % (12 pm-3 pm), 10 % (3 pm-6 pm), 30 % (6 pm-10 pm), 5 % (10 pm-12am)
Occupancy(Pers/m^2)	0.035[a] or 0.1[b,c]
Occupancy schedule: Dwellings Commercial areasOffices	% (10 pm-6am), 70 % (6am-8am), 20 % (8am-4 pm), 50 % (4 pm-6 pm) 90 % (6 pm-10 pm) 0 % (7 pm-8am), 10 % (8am-9am), 80 % (9am-1 pm), 30 % (1 pm-3 pm) 90 % (3 pm-7 pm) 0 % (6 pm-7am), 10 % (7am-9am), 90 % (9am-1 pm), 50 % (1 pm-2 pm) 90 % (2 pm-6 pm)
Appliances gain (W/m^2)	3[a] or 6[b,c]
Appliances gain schedule	7am-10pm[a] or 8.30am-12.30pm[b,c] and 3.30 pm-7pm[b,c]
Air change rate (Vol/h)	Infiltration 0.5[a,b,c] or Ventilation 1[b,c]
Air change rate schedule	Infiltration 24 h[a] 7 pm-7am[b,c] or Ventilation 7am-7pm[b,c]
Walls – U-value: A1950 1950–1975	cm), solid brick (38 cm), plaster (2 cm) – U = 1.34 W/m^2KPlaster (2 cm), semi solid brick (30 cm), plaster (2 cm) – U = 0.9 W/m2K
Windows U-value	Double – pane clear glass – U = 2.8 W/m^2K – SHGC = 0.75 (–)
Roof U-value: A1950 1950–1975	cm), tiles (2.5 cm) – U = 2.50 W/m^2KPlaster (2 cm), brick and concrete floor (24 cm), reinforced concrete (4 cm), tiles (2.5 cm) – U = 1.67 W/m^2K

referred to [a]dwellings, [b]commercial areas, [c]offices.

2.3. Proposed actions

In accordance with EPBD, the retrofit strategy must start from the reduction of the building demand through the use of passive techniques as much as possible and in particular the increase of the energy performance of the envelope.

The retrofit measures were categorized into three main groups, each aimed at systematically reducing non-renewable primary energy consumption. First, building envelope improvements were implemented to minimize heating and cooling loads, including the insulation of opaque surfaces and the replacement of existing windows. Next, high-efficiency energy generation systems, such as ASHP and GWHP, were introduced. Finally, renewable energy systems, such as BAPV and BIPV, were incorporated to offset residual energy demands. The methodological framework enabled a comprehensive assessment of each measure individually and in combination, considering both current and projected climatic conditions. Consequently, the first intervention analysis focused on the building envelope, as its insulation is a critical factor in reducing thermal losses. Two types of insulation were considered: external cladding (external insulation) and internal insulation, along with four different insulating materials: expanded polyurethane (EPS) [63], wood fiber [64], rock wool [65], and aerogel [66]. While external insulation offers better protection against weather conditions and enhances the building's thermal inertia, internal insulation may be preferable in contexts of architectural value or where facade characteristics must be preserved. Both insulation methods were evaluated for walls and roofs. For the four insulating materials, the thicknesses were selected to ensure compliance with the maximum thermal transmittance allowed by current Italian regulations [67]. In climate zone E (HDDs 2383), where Padua is located, the maximum allowed thermal transmittance is 0.26 W/m^2K for external walls and 0.22 W/m^2K for roofs. To achieve these values, the insulation thickness ranges from 18 cm (A1950 period with wood fiber) to 2 cm (1950–1975 period with aerogel) for roofs, while for walls, it varies from 16 cm (A1950 period with wood fiber) to 2 cm (1950–1975 period with aerogel). The choice of insulation material significantly influences the final thickness of the building structure. These materials exhibit distinct properties, such as density, specific heat capacity, and thermal conductivity. As a result, the thickness required to achieve a U-value in compliance with standards can vary significantly across different materials. While materials with similar U-values generally perform comparably under steady-state conditions, their differing thermophysical characteristics may influence results in dynamic simulations. To ensure a robust validation of the proposed retrofit strategies, thermal load calculations were conducted for each type of insulation material. As required by the aforementioned regulations, existing windows are replaced with new ones featuring a thermal transmittance of 1.3 W/m^2K and a Solar Heat Gain Coefficient (SHGC) of 0.54. For solar shading, reversible and architecturally compatible systems were assumed, with a modeling approach adaptable to both external blinds and traditional wooden shutters, which are commonly present or permitted in historic urban areas. In accordance with DIN 4108-2:2013 [68], solar shading devices were modeled with orientation- and use-specific activation thresholds (200–300 W/m^2 for residential and 150–200 W/m^2 for non-residential buildings), and with a solar transmittance factor (Fc) of 0.25 once activated. The shading system operates only during the cooling season, as shading is disabled in winter to allow passive solar gains and support heating needs.

The subsequent retrofit measures focus on the building systems. These interventions involve the use of reversible heat pumps for both heating and cooling. This entails replacing radiators with lower-temperature heating bodies. Specifically, radiant panel systems are planned for residential units, while fan coil units are expected to be installed in commercial and office buildings. During the winter season, the heat pumps operate with a design temperature difference of 45–40 °C in buildings equipped with fan coils and 35–30 °C where only radiant panels are present. DHW production requires heat at 50–45 °C. In summer, the temperature difference is 7–12 °C for fan coils and 10–15 °C for radiant panels.

The performance of the heat pumps was evaluated for each of the six archetype buildings using a dynamic simulation procedure of the building-system interaction, as detailed in a previous study [61]. This approach enabled the calculation of the hourly efficiencies of the heat pumps in heating, cooling, and DHW production for each category associated with an archetype building. Table 3 presents the obtained annual average values of the Coefficient of Performance (COP) for heating and DHW production, as well as the Energy Efficiency Ratio

Table 3
Annual average efficiencies for heating, cooling and DHW production in 2024.

Year 2024		COP	EER	DHW COP
ASHP	CR_A1950	3.6	4.1	3.4
	CR_1950-75	3.5	3.9	3.5
	CO_A1950	3.3	4.1	–
	CO_1950-75	3.2	3.8	–
	R_A1950	4.0	4.3	3.4
	R_1950-75	4.2	4.4	3.6
GWHP	CR_A1950	4.7	5.6	3.9
	CR_1950-75	4.5	5.4	3.8
	CO_A1950	4.3	5.2	–
	CO_1950-75	4.1	5.1	–
	R_1950	5.2	5.7	3.9
	R_1950-75	5.5	5.9	4.0

(EER) for cooling, derived from simulations using a 2024 climate file. For the boilers present in the baseline buildings, reference was made to the annual average value of thermal efficiency of 0.85 as specified by the national standard [68]. For cooling systems using air-cooled splits in the baseline scenario, simulations provided an average EER value of 3.6.

The dynamic building simulation calculates the hourly energy demand for heating, cooling, and DHW production. By dividing these energy demands by the corresponding efficiencies, the hourly thermal consumption of the boiler and the electrical consumption of the heat pumps can be determined. Additionally, the simulation model also provides hourly electrical consumption for lighting and plugged-in appliances.

To compare the performance of fossil fuel boilers with that of electric heat pumps, primary energy consumption must be considered. For electricity delivered by the public grid, the official Italian conversion factor [67], set at 2.42, is used. This factor comprises the contributions from the non-renewable portion (1.95) and the renewable portion (0.47) of energy produced by RES. Consequently, a final conversion factor of 1.95 is applied to calculate the non-renewable primary energy corresponding to the delivered electricity. This approach allows for the calculation of the building's annual hourly profile of primary energy demand, distinguishing between its renewable and non-renewable components.

Local renewable energy production is typically achieved through the installation of PV panels on the building's roof. In this study, the performance of two alternative PV technologies was assessed: traditional high-efficiency flat PV modules [69] and PV tiles [70]. PV tiles offer superior architectural and visual integration with existing roofs, but exhibit lower efficiency compared to flat modules. Table 4 summarizes the key characteristics of the two PV types, both of which utilize monocrystalline cells.

The performance of the PV system was simulated on an hourly time scale using the EnergyPlus PV model, which is based on the one-diode equivalent circuit model [71,72]. This model calculates the cell temperature using a dynamic approach developed by Ulleberg [73]. The one-diode model is a widely recognized method for simulating and analyzing the performance of photovoltaic (PV) modules. It characterizes the electrical behavior of a PV cell through an equivalent circuit comprising an ideal diode, a photocurrent source representing sunlight-generated current, a series resistance accounting for internal resistive losses, and a shunt resistance capturing leakage currents. Ulleberg's dynamic simulation method decouples the electrical and thermal properties of the PV cell, facilitating a more accurate determination of cell temperature. In this approach, cell temperature depends on its prior value and the thermal capacity of the module material. This methodology allows for precise performance simulation of PV systems under varying irradiance and temperature conditions. For each archetype building, the presence of a flat-panel PV system was assumed, designed to maximize coverage of all roof surfaces. Alternatively, the system was simulated using PV tiles, which can cover the entire roof area. In both cases, the PV system includes an electrical storage component based on lithium-ion batteries.

The dynamic hourly simulation of PV production and the building's electrical demand provides detailed hourly electricity flows, indicating grid consumption when demand exceeds production or surplus electricity when production exceeds demand. The storage capacity was dimensioned on a daily basis, considering the entire year. Specifically, the maximum daily surplus electricity was evaluated, representing the amount of energy produced by the PV panels that is not immediately consumed and, instead of being fed into the grid, can be stored in the battery for later use.

To simulate battery performance, a model based on the characteristics of a typical commercially available lithium-ion battery was used [74]. This reference battery provides 13.5 kWh of usable energy, with a maximum charge or discharge power of 5 kW and a round-trip efficiency of 90 %. For the storage system, instead of installing multiple identical batteries, a continuous variation in the installed usable energy capacity was assumed. However, the model maintained the ratio between maximum charge/discharge power and total usable energy equal to $5/13.5 = 0.37$.

At each time step, surplus PV production not immediately consumed by the building is used to charge the storage system, with any excess energy exported to the grid. When PV production falls short of the building's demand, the battery discharges as much energy as possible, with any remaining deficit supplied by the grid. The electric storage model operates on an hourly resolution, updating the stored energy level based on the initial state, net charge/discharge flux, round-trip efficiency, and maximum power exchange limits.

The dynamic simulation ultimately provides the annual non-renewable primary energy consumption for each of the six archetypes. For each archetype, this annual consumption is divided by the conditioned volume of the building, yielding a specific consumption value. Based on the adopted archetype method, the specific consumption is then multiplied by the total volume of buildings within the category represented by the given archetype. This calculation provides an estimate of the energy consumption for all buildings in that category. Summing the consumption of all categories yields the total energy consumption of all buildings analyzed within the study area. This procedure is repeated for the baseline scenario as well as for scenarios incorporating individual or combined interventions.

The complete set of analyzed interventions is presented in Table 5. Each action was evaluated individually or in combination with others to determine the specific contribution of each technology and the potential synergies arising from the adoption of integrated strategies for energy efficiency improvement. This integrated approach ensures a realistic evaluation of the combined effects of different strategies, avoiding overestimations or underestimations of their impact on energy performance.

A total of forty-two possible retrofit solutions were examined, each identified by a letter and numbers. These interventions are categorized into three main groups, each represented by a letter.

Table 4
Key characteristics of the two PV systems.

	Nominal Power	Nominal efficiency	Rated Voltage (Vmp)	Rated Current(Imp)	Open-Circuit Voltage (Voc)	Short-Circuit Current (Isc)	Surface
Flat PV module	400 W	22.5 %	65.8 V	6.08 A	75.6 V	6.58 A	1.798 m^2
PV tile	7.5 W	11.3 %	2.35 V	3.52 A	2.56 V	3.79 A	0.078 m^2

Table 5
The analyzed retrofit actions. the new u-values are also reported.

I: Envelope Insulation	G: Energy Generation System	R: Renewable Energy System
I1: Windows + Shading Systems ($U = 1.3\ W/m^2K$ – $SHGC = 0.54$)	**G1**: ASHP –	**R1**: PV flat panels + Batteries
I2: Wall – External Insulation ($U = 0.26\ W/m^2K$)	**G2**: GWHP	• **R1.1**: R1 + G3
• **I2.1**: EPS	**G3**: G1 + I5.4	• **R1.2**: R1 + G4
• **I2.2**: Wood fiber	**G4**: G2 + I5.4	• **R1.3**: R1 + G5
• **I2.3**: Rock wool	**G5**: G1 + I5.4 + I2.4	• **R1.4**: R1 + G6
• **I2.4**: Aerogel	**G6**: G2 + I5.4 + I2.4	• **R1.5**: R1 + G7
I3: Wall – Internal Insulation ($U = 0.26\ W/m^2K$)	**G7**: G1 + I6	• **R1.6**: R1 + G8
• **I3.1**: EPS	**G8**: G2 + I6	**R2**: PV Tiles + Batteries
• **I3.2**: Wood fiber		• **R2.1**: R2 + G3
• **I3.3**: Rock wool		• **R2.2**: R2 + G4
• **I3.4**: Aerogel		• **R2.3**: R2 + G5
I4: Roof – External Insulation ($U = 0.22\ W/m^2K$)		• **R2.4**: R2 + G6
• **I4.1**: EPS		• **R2.5**: R2 + G7
• **I4.2**: Wood fiber		• **R2.6**: R2 + G8
• **I4.3**: Rock wool		
• **I4.4**: Aerogel		
I5: Roof – Ceiling Insulation ($U = 0.22\ W/m^2K$)		
• **I5.1**: EPS		
• **I5.2**: Wood fiber		
• **I5.3**: Rock wool		
• **I5.4**: Aerogel		
I6: I1 + I2.4 + I5.4		

The letter I (Insulation) denotes various building envelope interventions, including replacing only the windows (I1) or insulating structures using four different types of insulating materials. Specifically, external wall insulation with a thermal cladding system (from I2.1 to I2.4), internal wall insulation with wall lining (from I3.1 to I3.4), roof insulation on the external side (from I4.1 to I4.4), or insulation of the uppermost floor slab (from I5.1 to I5.4). Finally, action I6 represents a combination of I1, I2.4, and I5.4.

The letter G (Generation) in the second group refers to the installation of heat pumps, where G1 and G2 indicate the installation of ASHPs (Air Source Heat Pumps) and GWHPs (Ground Water Heat Pumps), respectively. Combined interventions are also listed in this group.

The letter R (Renewable) introduces the use of PV flat panels (R1) and PV tiles (R2), along with their corresponding combined interventions.

It is important to emphasize that this study does not assume the universal applicability of all proposed retrofit solutions in every historic area. Instead, the approach is intended to assess the potential energy benefits of different strategies at a category level, offering valuable insights for policymakers and heritage authorities. The feasibility of each intervention in a specific building must be evaluated individually, taking into account architectural, structural, and regulatory constraints. This research aims to guide decision-making processes by identifying solutions that could align energy efficiency improvements with heritage preservation requirements, rather than determining the practical implementation of each measure in all cases.

2.4. Climate morphing

Meteorological data used in building energy simulations are commonly provided in the form of EPW (EnergyPlus Weather) files based on Typical Meteorological Years (TMY) [75]. TMY are synthetic datasets representing typical weather conditions for a given location, derived from historical climate data [76,77]. These datasets select the most meteorologically representative year for each month to provide a realistic, yet non-extreme, basis for simulations.

The EPW file considered as the current reference (i.e., EPW for 2024) in this study covers the period from 2007 to 2021 [78], as indicated in the databases of the National Centers for Environmental Information (NCEI) [79] and the ERA5 climate reanalysis [80]. Using current climate data, a climate morphing process was conducted to generate a 2050 climate file that accounts for ongoing climate change. The aim of this analysis is to assess the long-term effectiveness of the proposed set of interventions. The simulation was carried out using the Future Weather Generator software, developed by the University of Coimbra [81,82]. This software modifies existing hourly EPW files used in dynamic simulations to adapt them to climate change scenarios [83,84]. The software supports the five Shared Socioeconomic Pathways (SSPs) developed by the IPCC. To evaluate the long-term impact of the proposed retrofit interventions, the SSP5-8.5 scenario was chosen. This scenario represents the most pessimistic pathway among the five, characterized by limited technological progress and heavy reliance on fossil fuels. Policies are ineffective at reducing GHG emissions, leading to a significant increase in emissions and severe global environmental impacts. Based on this scenario, a 2050 EPW file was generated and used for simulations to compare with current climate conditions.

3. Outcomes

3.1. Benefits of retrofit actions under current climatic conditions

Fig. 5a–f illustrate the energy savings achieved through various efficiency interventions applied to different building categories within the study area. These savings are evaluated with reference to the consumption of non-renewable primary energy in the baseline condition. Specifically, the bar charts, referenced on the left y-axis, indicate the percentage savings relative to the total energy consumption of each building category. The figures also include a comparison with the 55 % threshold set by European directives as an initial step for energy retrofitting [13].

The analysis of the graphs reveals that envelope improvement interventions (I1–I5) result in savings below the 55 % threshold. Even cumulative interventions, such as I6, achieve a maximum of 47.5 % (CR_A1950). Among individual measures, window replacement (I1.1) has a limited impact, with savings ranging between 2.7 % and 7.9 %. External thermal insulation proves to be the most effective intervention, with savings up to 30 % in the mixed-use commercial and residential category (CR_1950–1976). However, the choice of insulation material (e.g., EPS, wood fiber, rock wool, or aerogel) shows variations of less than 1 %, suggesting that, given an equivalent final envelope thermal transmittance, the specific insulation material has a relatively minor impact on energy savings compared to the building's geometry and configuration.

Conversely, replacing generation systems emerges as a critical intervention. The installation of ASHPs provides savings ranging from 26.1 % to 43.1 % across various categories, while the more efficient GWHPs achieve savings between 33.5 % and 51.5 %. This underscores the importance of adopting advanced technologies to enhance the energy performance of existing buildings.

The effectiveness of combined interventions becomes evident when examining the synergy between envelope improvements and the replacement of generation systems. The highest savings were achieved by combining a high-efficiency envelope with heat pumps (G7 and G8), surpassing the 55 % threshold in four building categories.

The integration of PV systems, including both traditional modules and integrated PV tiles, represents an additional factor in energy efficiency, particularly in buildings with extensive roof surfaces and high electrical loads. In the analyzed cases, the combination of ASHPs and PV systems (R1.1 and R2.1) yielded energy savings ranging from 58.7 % to 76 %, significantly exceeding the 55 % target without requiring envelope interventions.

The comparison between traditional PV modules and PV tiles

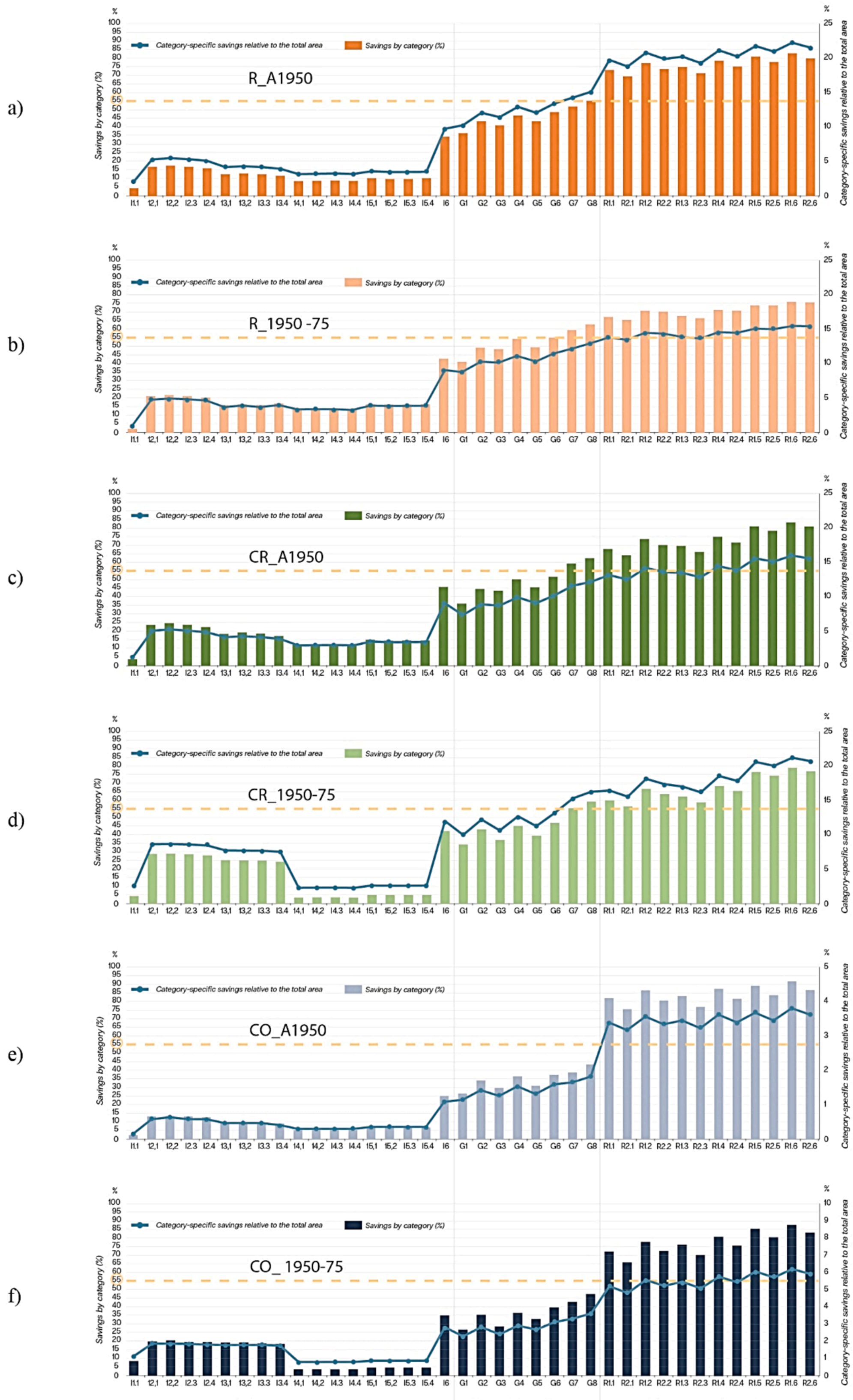

Fig. 5. Non-renewable primary energy savings achieved through interventions for each category, expressed as a percentage relative to the consumption of specific building categories or the total study are.

showed comparable results, as the ability to cover a larger roof area with tiles compensates for their lower efficiency relative to traditional modules.

Combined interventions, including envelope insulation, the installation of heat pumps, and PV systems, achieved savings exceeding 70 %, with a slight advantage for GWHPs paired with PV systems.

The curve in Fig. 5a to 5f, with values referenced on the right y-axis, illustrates the percentage savings achievable for each intervention within a given category, but now relative to the non-renewable primary energy consumption in the baseline condition of the whole study area. This metric is particularly significant for assessing the large-scale impact of interventions across all categories. Categories with lower volumetric incidence, such as CO_A1950, have a reduced impact, with savings limited to 4 % at the total area scale. Conversely, building categories such as CR_1950–1976 achieve savings of up to 20.6 % relative to the overall urban area consumption.

In Table 6, the non-renewable primary energy use (kWh/m^2) of the baseline buildings for the six archetypes is presented, along with the associated main combined interventions, subdivided by end-use. The table also includes the share of exported PV energy for each archetype.

The data from Table 6 offers deeper insight into which end uses benefit most from each intervention. For instance, envelope-focused measures (I6) notably reduce heating loads, while heat pump solutions (G7, G8) also impact cooling and DHW. Additionally, PV-based interventions (R1.6, R2.6) substantially lower electricity drawn from the grid. Overall, these numerical results highlight the percentage savings shown in Fig. 5, providing a direct reference to the absolute consumption levels for each scenario.

3.2. Projection of retrofit interventions to the 2050 climatic condition

Fig. 6a illustrates the monthly mean temperature trends for Padua in the years 2024 and 2050. Each month is represented by distinct box plots for 2024 and 2050, allowing a direct comparison of temperature distributions between the two time periods. The box plots provide a statistical summary of the temperature data: the central line represents the mean value, while the edges of the rectangle indicate the first and third quartiles (Q1 and Q3). Thus, the rectangle encompasses 50 % of the hourly temperature values for the month. The whiskers extend to show the range of minimum and maximum values, excluding potential outliers, which are represented as isolated points indicating extreme values excluded from the main range.

The analysis highlights a net increase in average and maximum temperatures between 2024 and 2050, consistent with the projections of the SSP5-8.5 scenario. During the winter months, a moderate rise in minimum temperatures is observed. In December, the minimum temperature increases from −9 °C in 2024 to −8.3 °C in 2050. The average winter temperature (January, February, March, November, and December) rises from 7.1 °C in 2024 to 9.0 °C in 2050, indicating moderate environmental warming. In summer, the temperature increase is more pronounced. In July, the average temperature rises from 25.3 °C in 2024 to 28.8 °C in 2050 (+3.5 °C). The maximum temperature, already high in 2024 (35.2 °C), reaches 39.2 °C in 2050, with an increase of 4 °C. The minimum temperature increases from 15.7 °C to 18.8 °C, signaling a rise in warm nights and a greater demand for cooling during evening hours. A similar trend is observed in August, with the average temperature rising from 25.9 °C in 2024 to 29.5 °C in 2050. The maximum temperature increases from 36.6 °C to 40.8 °C (+4.2 °C), marking the highest annual increment. The minimum temperature also increases, from 14.0 °C to 17.1 °C, confirming the necessity of continuous cooling to maintain indoor thermal comfort. Transition months, such as October and April, exhibit increases in average temperatures of 2.7 °C and 2.3 °C, respectively, suggesting a reduced demand for heating during these periods. In September, the average temperature rises from 20.0 °C in 2024 to 23.9 °C in 2050, while the maximum temperature increases from 32.0 °C to 36.2 °C (+4.2 °C), indicating an extended

Table 6
Non-renewable primary energy use (kWh/m^2) of the baseline buildings for the six archetypes, with associated main interventions subdivided by end-use. The total PV energy export share is also reported.

	R_A1950_3						R_1950–75_3					
	Baseline	I6	G7	G8	R1.6	R2.6	Baseline	I6	G7	G8	R1.6	R2.6
Heating	58.3	19.7	7.7	5.6	–-		103.5	31.4	12.2	8.9	–-	
Cooling	7.5	4.9	2.2	1.2			8.6	6.8	3.8	2.0		
DHW	18.5	17.9	8.2	7.1			18.0	17.2	7.9	6.9		
Lighting	13.4	11.9	11.9	11.9			16.2	15.4	15.4	15.4		
Appliances	26.0	25.2	25.2	25.2			25.4	24.3	24.3	24.3		
Net total (excluding used PV)					4.9	9.8					3.2	5.4
PV exported (kWh)					37,211	18,466					53,803	32,537
	CR_A1950_3						CR_1950_4					
	Baseline	I6	G7	G8	R1.6	R2.6	Baseline	I6	G7	G8	R1.6	R2.6
Heating	86.2	27.6	13.0	9.8	–-		90.9	25.4	12.0	9.0	–-	
Cooling	4.8	2.6	1.2	0.6			11.6	9.8	7.0	3.6		
DHW	9.7	9.0	4.1	3.6			15.5	15.0	6.9	6.0		
Lighting	12.6	11.7	11.7	11.7			12.5	11.6	11.6	11.6		
Appliances	26.7	25.0	25.0	25.0			33.3	32.5	32.5	32.5		
Net total (excluding used PV)					9.4	14.3					11.5	17.1
PV exported (kWh)					5932	2654					30,377	11,629
	CO_A1950_4						CO_1950–75_5					
	Baseline	I6	G7	G8	R1.6	R2.6	Baseline	I6	G7	G8	R1.6	R2.6
Heating	46.6	24.4	11.6	8.7	–-		43.4	14.5	6.9	5.1	–-	
Cooling	6.2	6.0	4.9	2.6			7.6	7.2	6.7	4.0		
DHW	–-	–-	–-	–-			–-	–-	–-	–-		
Lighting	14.0	13.9	13.9	13.9			8.7	8.7	8.7	8.7		
Appliances	30.7	30.3	30.3	30.3			30.4	29.6	29.6	29.6		
Net total (excluding used PV)					9.7	14.7					8.2	12.7
PV exported (kWh)					58,261	24,214					45,023	15,144

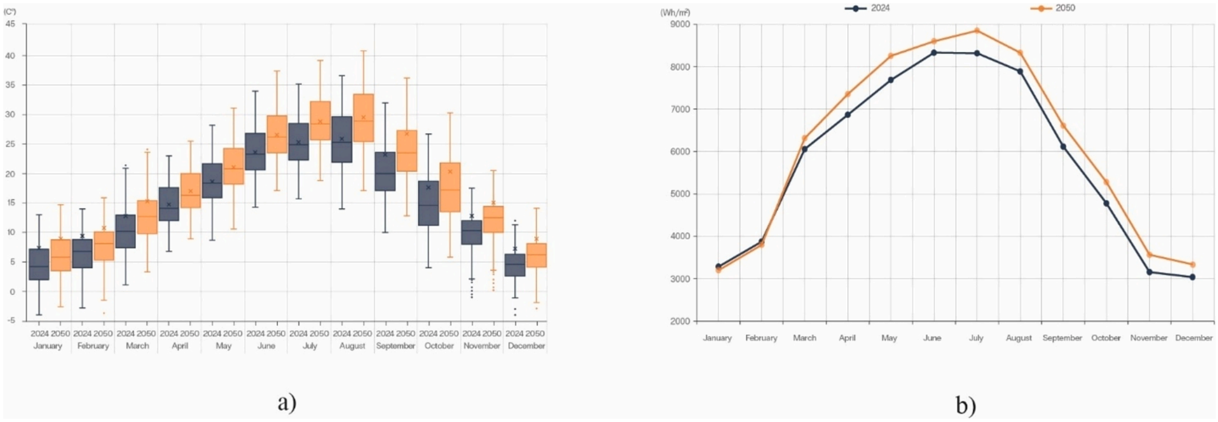

Fig. 6. Comparisons of box plots for monthly outdoor temperatures a) and monthly average daily solar radiation b) for the years 2024 and 2050.

cooling requirement. Finally, the box plots for 2050 show greater dispersion of values compared to 2024, highlighting an increase in climate variability. The interquartile range (IQR), which measures the difference between the first and third quartiles (Q1 and Q3), represents the central spread of the distribution and reflects the internal variability of the data. In August, the IQR increases from 7.7 °C in 2024 to 8.05 °C in 2050 (+4.5 %). In December, the IQR rises from 3.7 °C to 4.3 °C (+16.2 %). This increase in IQR suggests enhanced climate variability, with wider fluctuations between low and high temperatures. In summary, the comparison between 2024 and 2050 reveals significant warming across all seasons, with a more pronounced impact during summer months, especially on maximum temperatures. While winter shows moderate warming, it remains noteworthy. The greater dispersion observed in 2050 reflects increasing climate variability, with potential implications for thermal comfort and energy management. On an annual scale, the average outdoor air temperature rises from 14.9 °C in 2024 to 17.5 °C in 2050.

Fig. 6b illustrates the monthly average daily solar radiation, expressed in Wh/m^2, for Padua, comparing 2024 values with projections for 2050. The analysis indicates an increase in solar radiation in 2050 compared to 2024, particularly in spring and summer months. During summer (June to August), solar radiation increases, with values exceeding 8852 Wh/m^2 in 2050, compared to 8318 Wh/m^2 in 2024. This increase implies that in the summer of 2050, the solar energy incident on buildings will be significantly higher, resulting in a substantial rise in thermal load.

In detail:

- June: The monthly average daily solar radiation increases from approximately 8333 Wh/m^2 in 2024 to over 8601 Wh/m^2 in 2050.
- July: The maximum solar radiation peak occurs, rising from 8318 Wh/m^2 in 2024 to 8852 Wh/m^2 in 2050.
- August: An increase is observed from 7889 Wh/m^2 in 2024 to 8329 Wh/m^2 in 2050.
- This growth, combined with the rise in summer temperatures highlighted in the previous graph, reinforces the expectation that the energy demand for cooling buildings will be significantly higher in 2050.

During winter months, such as January, February, and December, solar radiation values remain relatively stable, with a slight increase between 2024 and 2050 but still at low levels, ranging between 3000 and 4000 Wh/m^2. For example:

- January: Solar radiation increases from approximately 3201 Wh/m^2 in 2024 to slightly over 3285 Wh/m^2 in 2050.
- December: An increase is observed from 3041 Wh/m^2 in 2024 to about 3339 Wh/m^2 in 2050.

This slight increase in solar radiation, coupled with the rise in winter temperatures, could help reduce the energy demand for heating buildings.

Using the 2050 EPW meteorological file, the building-plant system was re-simulated for each of the six archetype buildings. This approach enabled the evaluation of 2050 performance, which was then reassigned to the categories represented by the archetypes. Table 7 reports the average annual efficiencies of heat pumps evaluated under 2050 conditions. Regarding the simulations with ASHPs, the increase in temperature projected for 2050 results in an improvement in the COP and a decline in the EER, as expected. Concerning the simulations with GWHPs, the groundwater temperature in 2024 was assumed to average 15 °C, based on geological surveys conducted in the area [85]. This figure aligns with the Italian regulation [86], which estimates the average groundwater temperature to match the annual mean air temperature, recorded at 14.9 °C in 2024. For the GWHP simulations for 2050, the average groundwater temperature was assumed to equal the projected annual mean air temperature of 17.5 °C. Due to the proximity of these two temperatures, the calculated efficiencies for the two time periods exhibit minimal variation. Overall, the comparison between Tables 3 and 6 reveals no significant differences in COP and EER values calculated for 2024 and 2050. It can therefore be concluded that climate change does not substantially affect the performance of the evaluated heat pumps.

Fig. 7a compares the non-renewable primary energy consumption for the urban area under study in the current state, focusing on heating, cooling, miscellaneous electrical loads, and lighting for the years 2024 and 2050, based on the climate projections of the SSP5-8.5 scenario. The graph illustrates the annual consumption values, expressed in MWh, highlighting a significant transformation in their dynamics between 2024 and 2050. This change is primarily driven by the increase in

Table 7
Annual average efficiencies for heating, cooling and DHW production in 2050.

Year 2050		COP	EER	DHW COP
ASHP	CR_A1950	3.8	3.5	3.5
	CR_1950-75	3.7	3.3	3.6
	CO_A1950	3.4	3.6	–
	CO_1950-75	3.3	3.4	–
	R_A1950	4.3	3.7	3.5
	R_1950-75	4.4	3.9	3.6
GWHP	CR_A1950	4.9	5.4	4.2
	CR_1950-75	4.8	5.3	4.0
	CO_A1950	4.6	5.1	–
	CO_1950-75	4.5	5.0	–
	R_1950	5.6	5.6	4.1
	R_1950-75	5.8	5.8	4.2

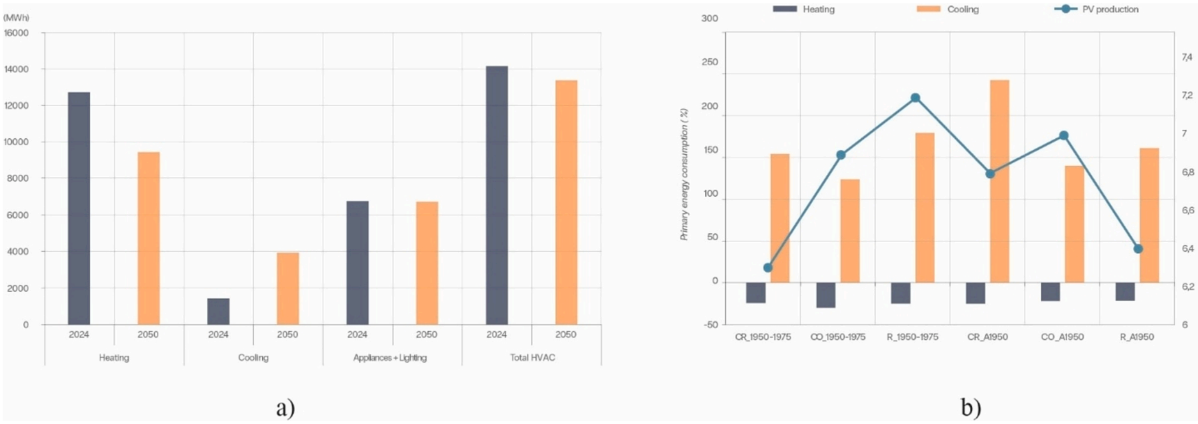

Fig. 7. Comparisons between 2050 and 2024: non-renewable primary energy consumption in the area a), percentage variations in heating, cooling consumption, and PV production across different categories b).

average temperatures and solar radiation, as shown in Fig. 6.

In 2024, the non-renewable primary energy consumption for heating is estimated at 12,717 MWh per year. By 2050, this value decreases by 25.7 %, dropping to 9,447 MWh, in line with the anticipated rise in winter temperatures under the SSP5-8.5 scenario, as indicated in Fig. 6a. This reduction reflects a diminished energy demand for maintaining thermal comfort during winter, significantly reducing heating system operating hours. Conversely, the non-renewable primary energy consumption for cooling experiences a sharp increase, rising from 1,439 MWh in 2024 to over 3,925 MWh in 2050, an increase of more than 270 %. This growth is closely linked to the substantial rise in summer temperatures and solar radiation, as previously discussed with reference to Fig. 6. Energy consumption related to lighting and miscellaneous electrical uses remains stable between 2024 and 2050, fluctuating around 6,700 MWh, indicating that these demands are not significantly affected by climate changes. In summary, the total energy consumption for climate control (heating and cooling) decreases, dropping from 14,157 MWh in 2024 to 13,372 MWh in 2050. However, this reduction conceals a substantial redistribution between seasonal loads. In 2024, cooling accounts for approximately 10.2 % of the total energy consumption for climate control; by 2050, this percentage increases to 29.4 %, indicating a structural shift in seasonal thermal loads. This change reflects a greater need for summer cooling compared to winter heating, with significant implications for the energy management of the analyzed buildings.

Fig. 7b illustrates the projected percentage changes by 2050 relative to 2024 for heating demand, cooling demand, and PV production across all building categories studied. The results clearly highlight the impact of climate change on energy needs and renewable energy production.

The consumption of non-renewable primary energy for heating undergoes a significant reduction across all building categories, with decreases ranging from 24.2 % to 29.9 %. In contrast, the consumption of non-renewable primary energy for cooling increases considerably, with increments between + 129.1 % and + 251.9 %. Regarding PV energy production, a moderate increase of 6.3 % to 7.2 % is observed, attributed to the rise in solar radiation (Fig. 6b). These data indicate that, although heating will require less energy by 2050, the substantial increase in cooling demand could pose significant challenges for energy resource management. The increase in PV production, while positive, may not be sufficient to offset the sharp rise in summer energy.

Based on the analysis of these data, a comprehensive study on the impacts of climate change on the planned interventions has been deemed essential to validate the long-term effectiveness of the selected energy strategies.

Fig. 8 illustrates the percentage savings achieved for each intervention, encompassing all building categories within the area. The figure compares the savings realized in 2024 with those anticipated for 2050, focusing on non-renewable primary energy consumption. The first histograms, from "I1.1″ to "I5.4," illustrate the energy savings associated with individual interventions on the building envelope. The replacement of windows (I1), combined with the installation of solar shading, results in a modest reduction in energy demand (4.3 % in 2024 and 3.7 % in 2050). However, this intervention alone is insufficient to significantly enhance overall thermal performance, highlighting heat losses through opaque surfaces and inefficiencies in generation systems. The insulation of walls, both external (I2) and internal (I3), shows a more significant improvement in energy performance, with savings ranging from 23.5 %

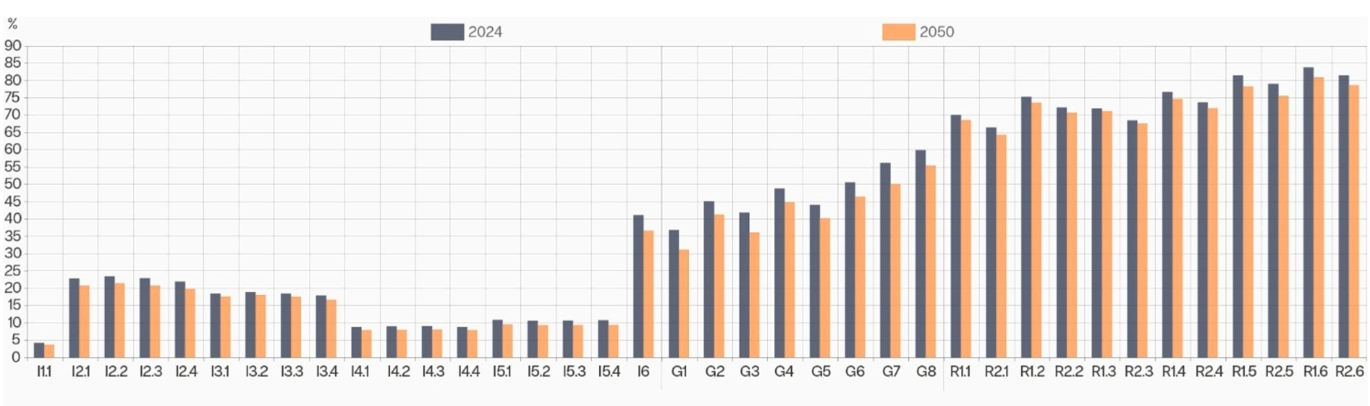

Fig. 8. Percentage savings achievable through the interventions relative to the non-renewable primary energy consumption of the entire area, evaluated for the years 2024 and 2050.

to 16.7 %, respectively. Similarly, roof insulation, whether external (I4) or internal (I5), contributes positively to reducing energy demand, with internal insulation exhibiting performance comparable to external insulation, yielding savings between 10.9 % and 8.0 %. The combined intervention (I6) achieves an overall reduction in energy demand of 41.1 % in 2024 and 36.7 % in 2050. This difference is attributed to the increase in winter temperatures, which negatively impacts the effectiveness of building envelope interventions in 2050.

The standalone replacement of the generation system with a ASHP (G1) results in a significant percentage savings of 36.9 % in 2024 and 31.2 % in 2050, without affecting the geometry of the building envelope. The introduction of a GWHP (G2) demonstrates excellent efficiency, with a reduction in energy demand of 45.2 % in 2024 and 41.4 % in 2050. The combinations integrating building envelope interventions with heat pumps (from G3 to G8) result in progressively greater savings. However, all values are slightly lower in 2050 compared to 2024. This is due to variations in the total demand for climate control, as previously observed in Fig. 7a for the baseline scenario, particularly the shift in demand between heating and cooling, coupled with the overall reduction in climate control demand. This reduction diminishes the relative advantage of heat pumps in 2050 compared to 2024.

The final set of histograms (R1.1 – R2.6) presents scenarios that include the installation of PV systems. These scenarios show an additional increase in achievable savings, ranging from a minimum of 64.5 % to a maximum of 83.9 %. In 2050, the improved performance of photovoltaics due to increased solar radiation reduces the gap in savings observed between 2024 and 2050. For example, the reduction in savings between 2024 and 2050 is 1.5 % (from 70.2 % to 68.7 %) in the R1.1 scenario, compared to 5.7 % (from 36.9 % to 31.2 %) in the G1 scenario. It is noteworthy that the installation of flat PV panels, despite being the most efficient, does not improve energy production and the resulting savings as expected. This limitation arises from the reduced PV surface area that can be covered with this type of solution. In contrast, PV tiles, although less efficient, allow for full surface coverage, achieving comparable savings.

The analysis highlights the importance of an integrated approach that combines advanced system technologies with renewable energy sources to reduce primary energy consumption both in 2024 and 2050. In particular, combinations involving GWHPs prove to be the most effective and are projected to deliver the highest savings even in 2050. Although the 2050 projections indicate significant climate changes and shifts in climate control demand, the findings underscore the importance of building efficiency improvements to manage energy consumption. The analyzed set of interventions remains effective in achieving this goal, even if implemented after 2024 and extending up to 2050.

4. Conclusion

The study focuses on the growing need for energy efficiency and sustainability in historic city center buildings, a particularly significant area for the preservation of cultural and architectural heritage. Energy retrofitting in these contexts faces a dual challenge: reducing energy consumption in compliance with European regulations while respecting historical constraints that limit invasive structural interventions on the building envelope.

The primary objective of this work was to analyze various energy retrofitting solutions, quantify their potential savings, and evaluate the effectiveness of each intervention to provide a decision-making tool for public administrations responsible for authorizing such projects. The simulations were conducted in a historic area of Padua's city center.

A key finding from the analysis is that interventions on the building envelope, such as window replacement and the insulation of façades and roofs, although architecturally impactful, have not proven to be the most effective in terms of overall energy savings. While these solutions are technically demanding, their energy efficiency has been relatively modest, especially when compared to system upgrades, which are significantly less invasive from an architectural perspective. The dynamic simulations showed modest yet discernible variations in performance, depending on the archetype, attributable to the use of different insulation materials. However, it is evident that while energy variations remain minimal, the architectural impact differs considerably due to the increased thickness of the building structure.

The replacement of boilers with heat pumps has demonstrated a significantly greater energy impact, especially when these machines utilize favorable cold sources, such as groundwater. The integration of electric heat pumps with rooftop PV systems equipped with electrical storage has further enhanced overall efficiency. Additionally, the use of PV tiles, which are less visually intrusive compared to traditional panels, has achieved similar results despite their lower nominal efficiency. This is due to the possibility of covering a larger roof area with PV tiles, given their smaller size.

The analysis of climate projections for 2050, based on the SSP5-8.5 scenario, has shown that the studied interventions remain valid even if implemented in 2050, thus proving effective in the face of significant climate changes anticipated during the 2024–2050 period. This highlights the role of energy retrofit strategies in enhancing the resilience of historic buildings, ensuring their long-term functionality and energy efficiency despite changing climatic conditions.

In this context, technological systems, particularly heat pumps coupled with PV systems, are confirmed as resilient technologies capable of maintaining high energy performance over the long term. The increased solar radiation expected in 2050 and the rise in cooling demand will further amplify the benefits of PV systems compared to current levels.

In conclusion, the study highlights that while modifications to the building envelope can improve energy performance, they are not always the most effective solutions, especially in historical contexts where architectural constraints limit the feasibility of such interventions. Advanced technological systems, such as heat pumps and photovoltaics, emerge as more efficient and sustainable approaches, particularly suited to addressing future climate changes expected by 2050. Implementation should also consider cost-effectiveness and durability: insulation typically lasts several decades, while heat pumps and PV systems need replacement after 15–30 years. Planning for maintenance and renewal is therefore essential, particularly in contexts where further interventions must be minimized. The best results are achieved through combined strategies that enhance both envelope performance and system efficiency, which should be regarded as complementary rather than alternative approaches. To support this integration, it will be crucial to define urban energy planning policies and regulations that promote the implementation of these technologies in existing buildings within historic centers. By integrating a detailed scenario-based analysis with a long-term perspective, this study provides valuable insights for decision-makers, supporting the development of interventions that are both effective and adaptable to the specific requirements of historic city centers. This will ensure an effective balance between energy efficiency and the preservation of architectural heritage, enabling redevelopment strategies that respond to the challenges posed by climate change.

CRediT authorship contribution statement

Luigi Schibuola: Writing – original draft, Conceptualization, Supervision, Methodology. **Mauro De Paris:** Visualization, Software, Data curation. **Paolo Di Micco:** Visualization, Software, Data curation. **Davide Roncarati:** Visualization, Software, Data curation. **Chiara Tambani:** Supervision, Investigation, Software, Data curation, Writing – original draft, Methodology, Conceptualization.

Declaration of competing interest

The authors declare that they have no known competing financial interests or personal relationships that could have appeared to influence

the work reported in this paper.

Appendix A. Supplementary data

Supplementary data to this article can be found online at https://doi.org/10.1016/j.enbuild.2025.116189.

Data availability

Data will be made available on request.

References

[1] Annual European Union greenhouse gas inventory 1990–2021 and inventory report 2023 Submission to the UNFCCC Secretariat https://www.eea.europa.eu/publications/annual-european-union-greenhouse-gas-2, (2023).
[2] Eurostat Database: https://ec.europa.eu/eurostat/databrowser/explore/all/envir?lang=en&subtheme=nrg.nrg_quant&display=list&sort=category.
[3] European Commission, Roadmap to a Resource Efficient Europe, communication: http://eur-lex.europa.eu/legal-content/EN/TXT/?uri=CELEX:52011DC0571, 2011.
[4] European Commission, In focus: energy efficiency in buildings: https://ec.europa.eu/info/news/focus-energy-efficiency-buildings-2020-lut-17.
[5] Factsheet, B. P. I. E. (2017). 97% of Buildings in the EU Need to Be Upgraded. Buildings Performance Institute Europe: Brussels, Belgium.
[6] P. Olasolo-Alonso, L.M. López-Ochoa, J. Las-Heras-Casas, L.M. López-González, Energy performance of buildings directive implementation in southern European countries: a review, Energy Build. 281 (2023) 112751, https://doi.org/10.1016/J.ENBUILD.2022.112751.
[7] C. Maduta, D. D'Agostino, S. Tsemekidi-Tzeiranaki, L. Castellazzi, G. Melica, P. Bertoldi, Towards climate neutrality within the European Union: assessment of the energy performance of buildings directive implementation in member states, Energy Build. 301 (2023) 113716, https://doi.org/10.1016/J.ENBUILD.2023.113716.
[8] European Commision, The European Green Deal: https://eur-lex.europa.eu/resource.html?uri=cellar:b828d165-1c22-11ea-8c1f-01aa75ed71a1.0002.02/DOC_1&format=PDF.
[9] L. Sandmann, E. Bülbül, R. Castaño-Rosa, F. Hanke, K. Großmann, R. Guyet, G. Jiglau, S. Laakso, E. Nuorivaara, A. Vornicu, The European Green Deal and its translation into action: multilevel governance perspectives on just transition, Energy Res. Soc. Sci. 115 (2024) 103659, https://doi.org/10.1016/J.ERSS.2024.103659.
[10] J. Ruiz, J.M. Martin-Moreno, R. Perez, Mid-term policy considerations of the EU green deal, Energ. Strat. Rev. 50 (2023) 101239, https://doi.org/10.1016/J.ESR.2023.101239.
[11] U. and G.A. Rebaudengo Manuela and Mecca, "Fit to 55": Financial Impacts of Italian Incentive Measures for the Efficiency of the Building Stock and the Revitalization of Fragile Areas, in: L. and P.M.M.J. Calabrò Francesco and Della Spina (Ed.), New Metropolitan Perspectives, Springer International Publishing, Cham, 2022: pp. 201–210.
[12] Thijs Vandenbussche, Is the EU's building renovation wave 'fit for 55'?, European Policy Centre (2021).
[13] European Commission, Fit for 55 : https://www.consilium.europa.eu/en/policies/fit-for-55/#:~:text=Fit%20for%2055%20refers%20to,line%20with%20the%202030%20goal.
[14] European commission: https://ec.europa.eu/commission/presscorner/detail/en/ip_23_4754.
[15] V. Costantini, C. Martini, B. Mini, M. Zoli, A Modified Environmental Kuznets Curve for Sustainable Development Assessment Using Panel Data, FEEM Working Paper No. 148.06 (2006).
[16] European Union, Energy Performance of Buildings Directive (EPBD), recast, 2024.
[17] E. Özer, I. Imamovic, L. Kranzl, G. Azzolini, S. Di Turi, F. Hugony, F. Zanghirella, National Building Renovation Plans and Zero-Emission Buildings Policy needs and best practices, 2024.
[18] L. Schibuola, M. Scarpa, C. Tambani, Innovative technologies for energy retrofit of historic buildings: an experimental validation, J. Cult. Herit. 30 (2018) 147–154, https://doi.org/10.1016/J.CULHER.2017.09.011.
[19] S. Lidelöw, T. Örn, A. Luciani, A. Rizzo, Energy-efficiency measures for heritage buildings: a literature review, Sustain. Cities Soc. 45 (2019) 231–242, https://doi.org/10.1016/J.SCS.2018.09.029.
[20] L. De Santoli, Guidelines on energy efficiency of cultural heritage, Energy Build. 86 (2015) 534–540, https://doi.org/10.1016/J.ENBUILD.2014.10.050.
[21] L. Celenza, M. Dell'Isola, G. Ficco, B.I. Palella, G. Riccio, Heat accounting in historical buildings, Energy Build. 95 (2015) 47–56, https://doi.org/10.1016/J.ENBUILD.2014.10.070.
[22] C. Panakaduwa, P. Coates, M. Munir, Identifying sustainable retrofit challenges of historical buildings: a systematic review, Energy Build. 313 (2024) 114226, https://doi.org/10.1016/J.ENBUILD.2024.114226.
[23] S.A. Sharbaf, P. Schneider-Marin, Cost-benefit analysis of sustainable upgrades in existing buildings: a critical review, Energy Build. 328 (2025) 115142, https://doi.org/10.1016/J.ENBUILD.2024.115142.
[24] I. Welch, The IPCC shared socioeconomic pathways (ssps): explained, evaluated, replaced, 2024.
[25] V. Masson-Delmotte, A. P. Zhai, S.L. Pirani, C. Connors, S. Péan, N. Berger, Y. Caud, L. Chen, M.I. Goldfarb, M. Gomis, K. Huang, E. Leitzell, J.B.R. Lonnoy, T.K. Matthews, T. Maycock, O. Waterfield, R. Yelekci, IPCC, 2021: Climate Change 2021: The Physical Science Basis. Contribution of Working Group I to the Sixth Assessment Report of the Intergovernmental Panel on Climate Change, 2021. https://doi.org/doi:10.1017/9781009157896.
[26] J. Rogelj, A. Popp, K.V. Calvin, G. Luderer, J. Emmerling, D. Gernaat, S. Fujimori, J. Strefler, T. Hasegawa, G. Marangoni, V. Krey, E. Kriegler, K. Riahi, D.P. van Vuuren, J. Doelman, L. Drouet, J. Edmonds, O. Fricko, M. Harmsen, P. Havlík, F. Humpenöder, E. Stehfest, M. Tavoni, Scenarios towards limiting global mean temperature increase below 1.5 °C, Nat. Clim. Change. 8 (2018) 325–332, https://doi.org/10.1038/s41558-018-0091-3.
[27] K. Riahi, D.P. van Vuuren, E. Kriegler, J. Edmonds, B.C. O'Neill, S. Fujimori, N. Bauer, K. Calvin, R. Dellink, O. Fricko, W. Lutz, A. Popp, J.C. Cuaresma, M. Leimbach, L. Jiang, T. Kram, S. Rao, J. Emmerling, K. Ebi, T. Hasegawa, P. Havlik, F. Humpenöder, L.A. Da Silva, S. Smith, E. Stehfest, V. Bosetti, J. Eom, D. Gernaat, T. Masui, J. Rogelj, J. Strefler, L. Drouet, V. Krey, G. Luderer, M. Harmsen, K. Takahashi, L. Baumstark, J.C. Doelman, M. Kainuma, Z. Klimont, G. Marangoni, H. Lotze-Campen, M. Obersteiner, A. Tabeau, M. Tavoni, The shared socioeconomic pathways and their energy, land use, and greenhouse gas emissions implications: an overview, Glob. Environ. Chang. 42 (2017) 153–168, https://doi.org/10.1016/J.GLOENVCHA.2016.05.009.
[28] M.P. Tootkaboni, I. Ballarini, M. Zinzi, V. Corrado, A comparative analysis of different future weather data for building energy performance simulation, Climate 9 (2021), https://doi.org/10.3390/cli9020037.
[29] Z. Duan, P. de Wilde, S. Attia, J. Zuo, Prospect of energy conservation measures (ECMs) in buildings subject to climate change: a systematic review, Energy Build. 322 (2024) 114739, https://doi.org/10.1016/J.ENBUILD.2024.114739.
[30] G. Tomrukcu, T. Ashrafian, Climate-resilient building energy efficiency retrofit: evaluating climate change impacts on residential buildings, Energy Build. 316 (2024) 114315, https://doi.org/10.1016/J.ENBUILD.2024.114315.
[31] C. Citadini de Oliveira, I. Catão Martins Vaz, E. Ghisi, Retrofit strategies to improve energy efficiency in buildings: an integrative review, Energy Build. 321 (2024) 114624, https://doi.org/10.1016/J.ENBUILD.2024.114624.
[32] M. Ibrahim, F. Harkouss, P. Biwole, F. Fardoun, S. Ouldboukhitine, Building retrofitting towards net zero energy: a review, Energy Build. 322 (2024) 114707, https://doi.org/10.1016/J.ENBUILD.2024.114707.
[33] A.S. Gaur, D.Z. Fitiwi, J. Curtis, Heat pumps and our low-carbon future: a comprehensive review, Energy Res. Soc. Sci. 71 (2021) 101764, https://doi.org/10.1016/J.ERSS.2020.101764.
[34] U. Berardi, S. Jones, The efficiency and GHG emissions of air source heat pumps under future climate scenarios across Canada, Energy Build. 262 (2022) 112000, https://doi.org/10.1016/J.ENBUILD.2022.112000.
[35] M.H. Abbasi, B. Abdullah, M.W. Ahmad, A. Rostami, J. Cullen, Heat transition in the European building sector: overview of the heat decarbonisation practices through heat pump technology, Sustainable Energy Technol. Assess. 48 (2021) 101630, https://doi.org/10.1016/J.SETA.2021.101630.
[36] M. Chesser, P. Lyons, P. O'Reilly, P. Carroll, Air source heat pump in-situ performance, Energy Build. 251 (2021) 111365, https://doi.org/10.1016/J.ENBUILD.2021.111365.
[37] Y. Jung, J. Oh, U. Han, H. Lee, A comprehensive review of thermal potential and heat utilization for water source heat pump systems, Energy Build. 266 (2022) 112124, https://doi.org/10.1016/J.ENBUILD.2022.112124.
[38] L. Schibuola, C. Tambani, Performance assessment of seawater cooled chillers to mitigate urban heat island, Appl. Therm. Eng. 175 (2020) 115390, https://doi.org/10.1016/J.APPLTHERMALENG.2020.115390.
[39] L. Schibuola, C. Tambani, A. Buggin, Seawater opportunities to increase heating, ventilation, and air conditioning system efficiency in buildings and urban resilience, Front. Energy Res. 10 (2022), https://doi.org/10.3389/fenrg.2022.913411.
[40] A. Galgaro, M. Cultrera, Thermal short circuit on groundwater heat pump, Appl. Therm. Eng. 57 (2013) 107–115, https://doi.org/10.1016/J.APPLTHERMALENG.2013.03.011.
[41] D. Milenić, P. Vasiljević, A. Vranješ, Criteria for use of groundwater as renewable energy source in geothermal heat pump systems for building heating/cooling purposes, Energy Build. 42 (2010) 649–657, https://doi.org/10.1016/J.ENBUILD.2009.11.002.
[42] L. Schibuola, C. Tambani, A. Zarrella, M. Scarpa, Ground source heat pump performance in case of high humidity soil and yearly balanced heat transfer, Energy Convers. Manage. 76 (2013) 956–970, https://doi.org/10.1016/J.ENCONMAN.2013.09.002.
[43] J. Stock, T. Schmidt, A. Xhonneux, D. Müller, Optimisation of district heating transformation for the efficient integration of a low-temperature heat source, Energy 308 (2024) 132461, https://doi.org/10.1016/J.ENERGY.2024.132461.
[44] M. Alhuyi Nazari, J. Rungamornrat, L. Prokop, V. Blazek, S. Misak, M. Al-Bahrani, M.H. Ahmadi, An updated review on integration of solar photovoltaic modules and heat pumps towards decarbonization of buildings, Energy Sustain. Dev. 72 (2023) 230–242, https://doi.org/10.1016/J.ESD.2022.12.018.
[45] L. Schibuola, M. Scarpa, C. Tambani, Influence of charge control strategies on electricity import/export in battery-supported photovoltaic systems, Renew. Energy 113 (2017) 312–328, https://doi.org/10.1016/J.RENENE.2017.05.089.
[46] L. Schibuola, M. Scarpa, C. Tambani, Demand response management by means of heat pumps controlled via real time pricing, Energy Build. 90 (2015) 15–28, https://doi.org/10.1016/J.ENBUILD.2014.12.047.

[47] N. Aste, C. Del Pero, F. Leonforte, S. Ounis, A.M.G. Abdelrahim, The role of photovoltaic technology in achieving net zero energy target in residential buildings, Energ. Strat. Rev. 55 (2024) 101543, https://doi.org/10.1016/J.ESR.2024.101543.
[48] L.K. Wiginton, H.T. Nguyen, J.M. Pearce, Quantifying rooftop solar photovoltaic potential for regional renewable energy policy, Comput. Environ. Urban Syst. 34 (2010) 345–357, https://doi.org/10.1016/J.COMPENVURBSYS.2010.01.001.
[49] M. Ashraf Fauzi, N. Hanis Zainal Abidin, N. Mohd Suki, A. Mokhtar Albshir Budiea, Residential rooftop solar panel adoption behavior: bibliometric analysis of the past and future trends, Renew. Energy Focus 45 (2023) 1–9, https://doi.org/10.1016/J.REF.2023.02.002.
[50] L. Ding, Y. Zhu, L. Zheng, Q. Dai, Z. Zhang, What is the path of photovoltaic building (BIPV or BAPV) promotion? –the perspective of evolutionary games, Appl. Energy 340 (2023) 121033, https://doi.org/10.1016/J.APENERGY.2023.121033.
[51] A. Ghosh, Potential of building integrated and attached/applied photovoltaic (BIPV/BAPV) for adaptive less energy-hungry building's skin: a comprehensive review, J. Clean. Prod. 276 (2020) 123343, https://doi.org/10.1016/J.JCLEPRO.2020.123343.
[52] L.F. Cabeza, A. de Gracia, A.L. Pisello, Integration of renewable technologies in historical and heritage buildings: a review, Energy Build. 177 (2018) 96–111, https://doi.org/10.1016/J.ENBUILD.2018.07.058.
[53] T.E. Kuhn, C. Erban, M. Heinrich, J. Eisenlohr, F. Ensslen, D.H. Neuhaus, Review of technological design options for building integrated photovoltaics (BIPV), Energy Build. 231 (2021) 110381, https://doi.org/10.1016/J.ENBUILD.2020.110381.
[54] D.S. Pillai, V. Shabunko, A. Krishna, A comprehensive review on building integrated photovoltaic systems: emphasis to technological advancements, outdoor testing, and predictive maintenance, Renew. Sustain. Energy Rev. 156 (2022) 111946, https://doi.org/10.1016/J.RSER.2021.111946.
[55] L.G. Swan, V.I. Ugursal, Modeling of end-use energy consumption in the residential sector: a review of modeling techniques, Renew. Sustain. Energy Rev. 13 (2009) 1819–1835, https://doi.org/10.1016/J.RSER.2008.09.033.
[56] X. Yang, M. Hu, N. Heeren, C. Zhang, T. Verhagen, A. Tukker, B. Steubing, A combined GIS-archetype approach to model residential space heating energy: a case study for the Netherlands including validation, Appl. Energy 280 (2020) 115953, https://doi.org/10.1016/J.APENERGY.2020.115953.
[57] DesignBuilder Software Ltd, DesignBuilder v 7.3 https://designbuilder.co.uk.
[58] U.S. Department of Energy, EnergyPlus, Https://Energyplus.Net/. (2019).
[59] G. Peri, L. Cirrincione, D. Mazzeo, N. Matera, G. Scaccianoce, Building resilience to a warming world: a contribution toward a definition of "integrated climate resilience" specific for buildings - literature review and proposals, Energy Build. 315 (2024) 114319, https://doi.org/10.1016/J.ENBUILD.2024.114319.
[60] K. Riahi, S. Rao, V. Krey, C. Cho, V. Chirkov, G. Fischer, G. Kindermann, N. Nakicenovic, P. Rafaj, RCP 8.5—A scenario of comparatively high greenhouse gas emissions, Clim. Change 109 (2011) 33, https://doi.org/10.1007/s10584-011-0149-y.
[61] L. Schibuola, C. Tambani, Non-renewable energy demand reduction and positive energy buildings in Southern Europe's urban forms, Energy Build. 328 (2025) 115185, https://doi.org/10.1016/J.ENBUILD.2024.115185.
[62] UNI/TR 11552, Abaco delle strutture costituenti l'involucro opaco degli edifici. Parametri termo fisici, tecnica report, 2014.
[63] Expanded polystyrene thermal insulation panels, https://www.fassabortolo.co.uk/documents/10179/2102698/FASSAUK_STE_EN_WHITE-EPS-70-RAIL-SYSTEM-UK_2020-03.pdf/f487a6bd-a99b-4653-95a5-04218302b707.
[64] Wood fibre insulation board, https://www.betonwood.com/eng/pdf/Data_sheet_wood_fiber_fibertherm_protectdry180.pdf.
[65] Rock mineral wool slab, https://www.fassabortolo.co.uk/documents/10179/2783525/FASSAUK_STE_EN_EWI-DUAL-DENSITY-SLAB_2021-03.pdf/ac3f3cec-b81e-4589-9f23-4502b93921f3.
[66] Silica aerogel panel, https://aeropan.it/en/service/amagel-a2-en/.
[67] DM 26 giugno 2015, Applicazione delle metodologie di calcolo delle prestazioni energetiche e definizione delle prescrizioni e dei requisiti minimi degli edifici, 2015.
[68] DIN 4108-2:2013 Thermal protection and energy economy in buildings Part 2: Minimum requirements to thermal insulation. Deutsches Institut für Normung e.V. (DIN), Berlin, 2013.
[69] Maxeon SunPower 3 400 W, Https://Sunpower.Maxeon.Com/Au/Sites/Default/Files/2019-07/Max3-400-390-370-Au_0.Pdf.
[70] Photovoltaic Rooftile, https://www.invisiblesolar.it/EN/wp-content/uploads/2024/09/Technical-Booklet-IS001-2.1-2024-rev.02-EN.pdf, n.d.
[71] J.H. Eckstein, Detailed Modelling of Photovoltaic System Components, 1990.
[72] J.A. Duffie, W.A. Beckman, Solar Engineering of Thermal Processes, 2013.
[73] Ø. Ulleberg, HYDROGEMS Component Library for TRNSYS 15 User Manual, 2001.
[74] Tesla Powerwall, https://www.tesla.com/sites/default/files/pdfs/powerwall/Powerwall%202_AC_Datasheet_en_AU.pdf.
[75] I.J. Hall, R.R. Prairie, H.E. Anderson, E.C. Boes, Generation of a typical meteorological year Sandia Labs, Albuquerque, NM (USA) (1978).
[76] G. Evola, V. Costanzo, M. Infantone, L. Marletta, Typical-year and multi-year building energy simulation approaches: a critical comparison, Energy 219 (2021) 119591, https://doi.org/10.1016/J.ENERGY.2020.119591.
[77] C.Y. Siu, Z. Liao, Is building energy simulation based on TMY representative: a comparative simulation study on doe reference buildings in Toronto with typical year and historical year type weather files, Energy Build. 211 (2020) 109760, https://doi.org/10.1016/J.ENBUILD.2020.109760.
[78] climate.onebuilding.org, https://climate.onebuilding.org/.
[79] National Centers for Environmental Information (NCEI), https://www.ncei.noaa.gov/.
[80] ECMWF Reanalysis v5 (ERA5), https://www.ecmwf.int/en/forecasts/dataset/ecmwf-reanalysis-v5.
[81] Future Weather Generator software, https://future-weather-generator.adai.pt/.
[82] E. Rodrigues, M.S. Fernandes, D. Carvalho, Future weather generator for building performance research: an open-source morphing tool and an application, Build. Environ. 233 (2023) 110104, https://doi.org/10.1016/J.BUILDENV.2023.110104.
[83] I. Tajuddeen, E. Rodrigues, A Morris sensitivity analysis of an office building's thermal design parameters under climate change in sub-Saharan Africa, Build. Environ. 262 (2024) 111771, https://doi.org/10.1016/J.BUILDENV.2024.111771.
[84] C. Rodrigues, E. Rodrigues, M.S. Fernandes, S. Tadeu, Prospective life cycle approach to buildings' adaptation for future climate and decarbonization scenarios, Appl. Energy 372 (2024) 123867, https://doi.org/10.1016/J.APENERGY.2024.123867.
[85] ARPAV, Le acque sotterranee della Regione Veneta, https://www.arpa.veneto.it/temi-ambientali/acque-interne/acque-interne/acque-sotterranee/sai_rsgw_2008.pdf/@@display-file/file.
[86] UNI/TS 11300:2, Energy Performance of Buildings, Technical Specification, Italian standard, 2014.